EXPERIMENTAL INVESTIGATION OF ULTRA-HIGH VACUUM ADHESION AS RELATED TO THE LUNAR SURFACE

SIXTH QUARTERLY PROGRESS REPORT

1 OCTOBER THROUGH 31 DECEMBER 1965

J. A. Ryan
Principal Investigator
R&D/Lunar and Planetary
Sciences Branch

Prepared for:
NASA Office of
Advanced Research & Technology
Washington, D. C.

Contract NAS 7-307

Date of Issue:
26 June 1964
A-830-BBK3-2

MISSILE & SPACE SYSTEMS DIVISION
DOUGLAS AIRCRAFT COMPANY, INC.
SANTA MONICA, CALIFORNIA

TABLE OF CONTENTS

	Page
1.0 INTRODUCTION	1
2.0 EXPERIMENTAL	2
2.1 Vacuum System Modifications	2
2.1.1 Sorption Pump Bank	2
2.1.2 Second Vacuum Chamber	2
2.1.3 Cleavage Device	3
2.2 Experimental Data	4
3.0 DISCUSSION	18
3.1 Effects of Forepump Type	18
3.2 Repeatability	20
3.3 Orientation Effects	20
3.4 Roughness Effects	21
3.5 Material Transfer	22
4.0 SUMMARY	23
REFERENCE	24

1.0 INTRODUCTION AND SUMMARY

This report presents a summary of the work accomplished during the period October through December, 1965, on the study of the ultra-high vacuum frictional-adhesional behavior of silicates as related to the lunar surface.

During this period, the mechanical forepump utilized during the previous quarters was replaced by a sorption pump bank. Also, the original vacuum chamber was replaced by a second chamber which permits utilization of an electron gun, and allows vacuum cleavage operations to be performed. Finally, preliminary development of a device permitting vacuum cleavage was completed.

Investigations were made as to (1) the effects of forepump type upon the data obtained, (2) data repeatability, (3) orientation effects, and (4) surface roughness effects.

Data were obtained for orthoclase (001) contacting orthoclase (001) for various surface roughnesses and crystalline orientations; and for orthoclase (001) contacting hypersthene (110). Orientation effects were noted, but these have not as yet been conclusively related to crystalline structure. It was found, also, that surface roughness had no apparent effect on Type A adhesion (believed to be produced through the action of the normal lattice bonding forces), but that decreasing surface roughness produced an increase in the magnitude of Type B adhesion (probably produced through the action of dispersion forces). Additionally, it was found that replacement of the mechanical pump with sorption pumps had no effect on the ultra-high vacuum adhesional behavior observed. Finally, it was found that the adhesional data had a reasonably good repeatability.

2.0 EXPERIMENTAL

2.1 Vacuum System Modifications

2.1.1. Sorption Pump Bank

All data from the previous quarters were obtained with a well-trapped mechanical pump as the forepump. Though, as noted in the last quarterly report, great care was used to ensure that no oil back-streamed into the ultra-high vacuum part of the system, it was decided to replace this possible source of contamination with sorption pumps. Accordingly, a sorption pump bank was assembled and placed into operation at the beginning of this quarter.

The bank consists of three standard sorption pumps with associated heaters and liquid nitrogen dewars, a Pirani gage for pressure monitoring, three valves for individual pump control, and a fourth valve for admittance of dry nitrogen to the system. The manifold for the system was constructed of 304 stainless steel, and the entire assembly was mounted on a cart permitting the assembly to be detached from the ultra-high vacuum part of the system during the experiment. With these sorption pumps it was found that the system could be pumped from atmospheric pressure to ion pump start pressure in 20-30 minutes.

2.1.2 Second Vacuum Chamber

The experimental chamber used since the beginning of the study was, during this quarter, replaced by a second chamber. The primary purposes of this change were to permit utilization of an electron gun for surface cleaning, and to allow vacuum cleavage to be performed. The basic modifications were to (1) expand the vertical height of the chamber, and add additional bellows, so that the samples could be separated sufficiently for the electron gun to be inserted between them, and (2) provide additional ports for the electron gun and the cleavage apparatus. Other modifications were (1) the addition of more view ports to aid in the observation of the samples and the microbalance, (2) the improvement of the micrometer screws attached to the tilt stage to reduce the problems associated with obtaining sample parallelism, and (3) polishing the interior chamber walls to aid in obtaining better vacuum.

This new chamber has operated successfully during this quarter. With it, lower base pressures have been obtained ($\cong 1 \times 10^{-10}$ mm Hg). Neither the electron gun nor the cleavage device have as yet been inserted into the chamber. However, it is expected that this will be done during the next quarter.

2.1.3 Cleavage Device

The cleavage device consists basically of a tool steel chisel and a sample holder. The purpose of the chisel is to produce the cleavage. It is wedge-shaped and formed to fit into a pre-cut small slot in the sample. The chisel is mounted on bellows so that it can be brought into contact with the sample for cleavage and then withdrawn prior to measurement of adhesion. Cleavage is produced by impacting the chisel from outside the chamber. The purpose of the sample holder is to hold the sample rigidly during cleavage, thereby preventing damage to the microbalance. It is designed to fit around the metal bucket (used to apply load force) so that the load force dependence of the adhesion can be measured. The holder can be removed (by means of bellows) from the vicinity of the sample after cleavage has been accomplished.

This system has been tested in air and found to perform well. The cleavage faces produced to date have not been perfect, though they have generally been satisfactory. It is believed that with practice excellent faces can be produced. The first vacuum cleavage attempts will be made during the next quarter.

2.2 Experimental Data

Adhesion versus load data were obtained for orthoclase (001) contacting orthoclase (001) for four crystalline orientations and with different surface roughnesses; and for orthoclase (001) contacting hypersthene (110). The roughness plots for the orthoclase samples are shown in Figures 1-6. Figures 7 and 8 show roughness plots for the orthoclase samples used in Runs #17 and #18 of the previous quarter [Note: in the previous report these samples were erroneously labeled O(//)3T and O(//)2B]. These latter plots are reproduced here for purposes of discussion of the data obtained during the present quarter. The roughness plots for the hypersthene and the orthoclase used with it are given in Reference 1. Table 1 gives the pertinent data regarding the experimental conditions.

TABLE 1
EXPERIMENTAL CONDITIONS

Run No.	Top Sample	Bottom Sample	Vacuum (mmHg)	Comments
19	Orthoclase(001) O(//)4T	Orthoclase (001) O(//)4B	4×10^{-10}	a-AXIS/a-AXIS = 100°
20	Orthoclase(001) O(//)4T	Orthoclase(001) O(//)4B	4×10^{-10}	a-AXIS/a-AXIS = 190°
21	Orthoclase (001) O(//)F1	Orthoclase (001) O(//)F2	3×10^{-10}	a-AXIS/a-AXIS = 90°
22	Hypersthene (110) Hs(//)NP	Orthoclase (001) O(//)2T	1×10^{-10}	a-AXIS TRACE/a-AXIS = 15°

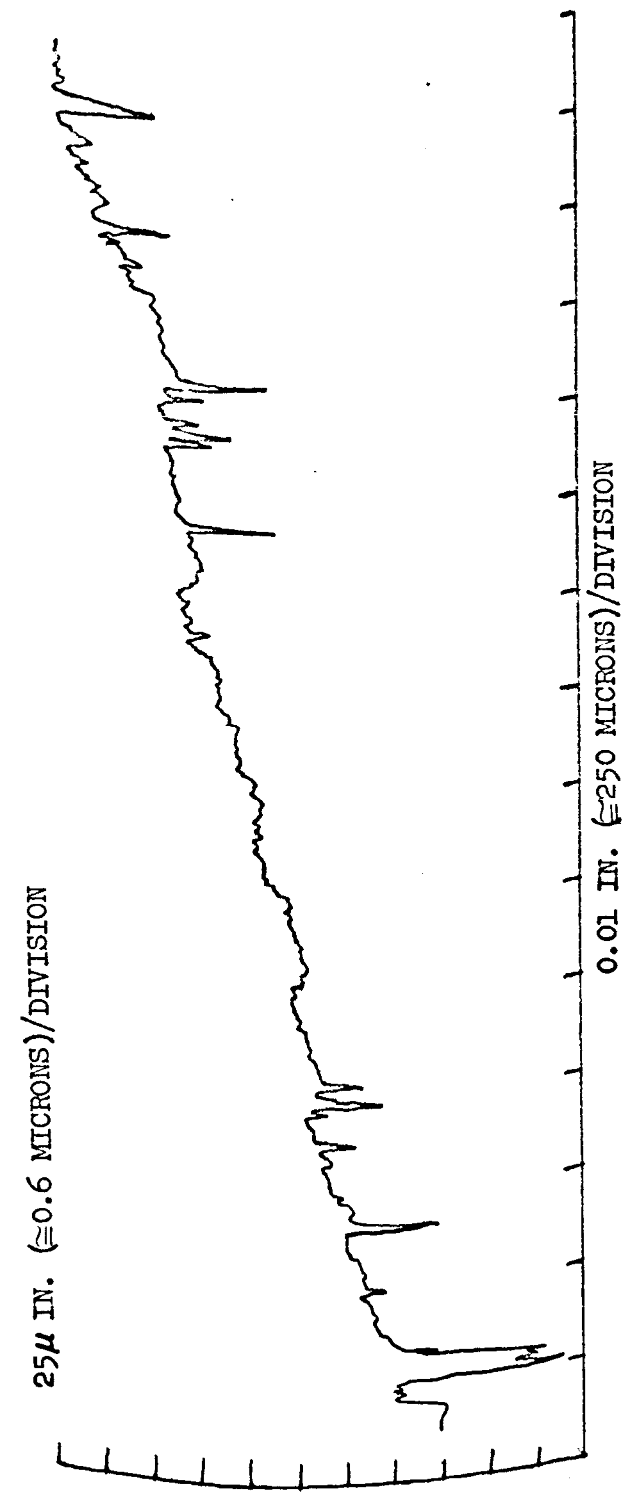

ORTHOCLASE (001)

o(//) 4T

SURFACE ROUGHNESS

ALONG a-AXIS

Figure 1

ORTHOCLASE (001)

0(//) 4T

SURFACE ROUGHNESS

ALONG b-AXIS

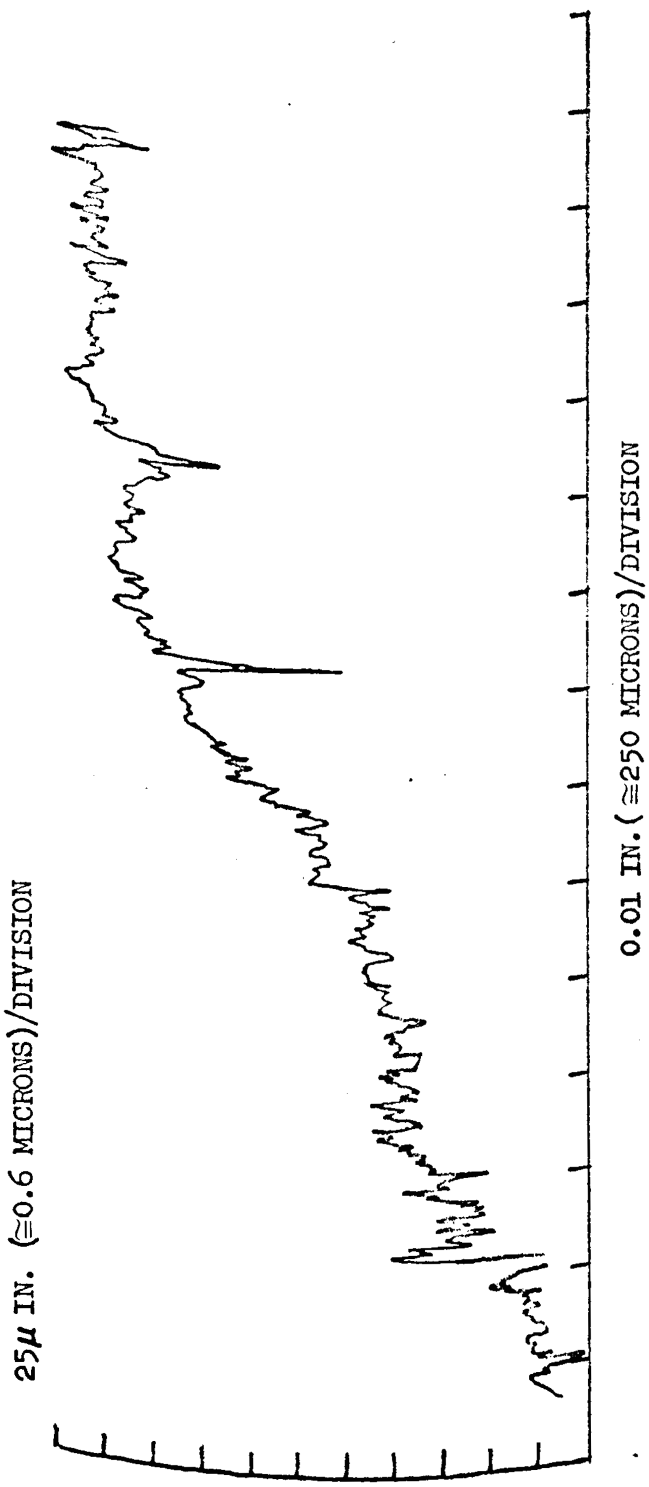

Figure 2

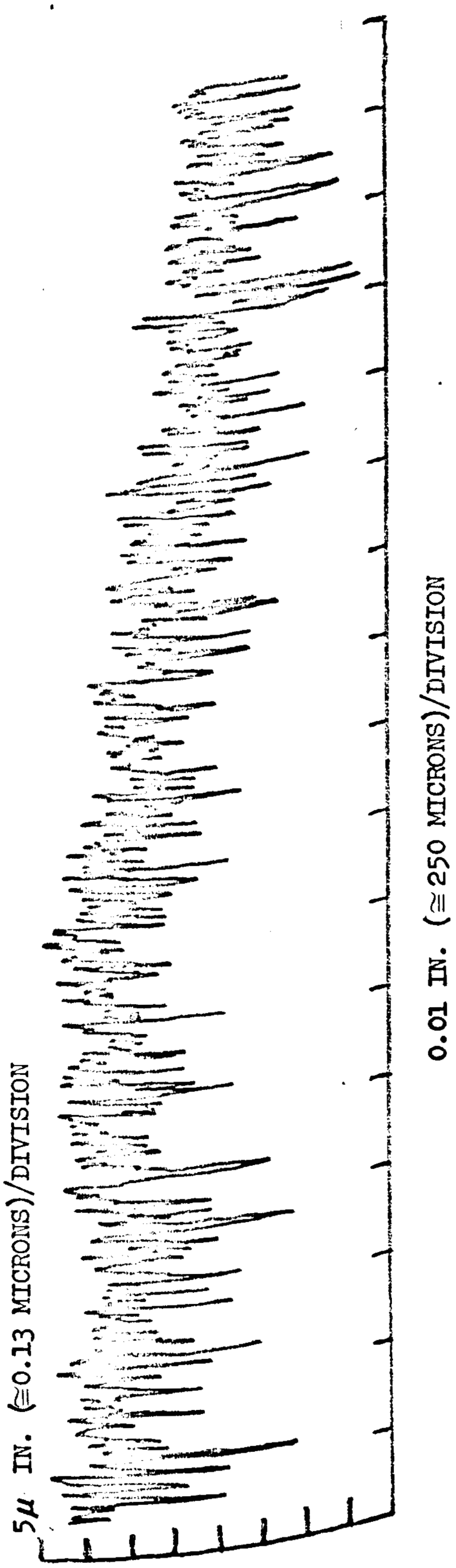

ORTHOCLASE (001)

O(//) 4B

SURFACE ROUGHNESS

ALONG a-AXIS

Figure 3

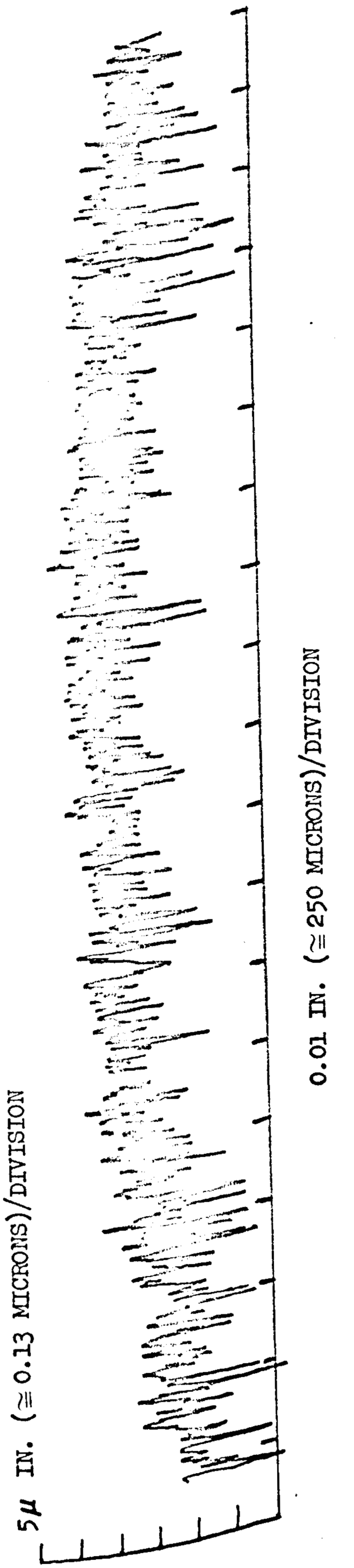

ORTHOCLASE (001)

O(//) 4B

SURFACE ROUGHNESS

ALONG b-AXIS

Figure 4

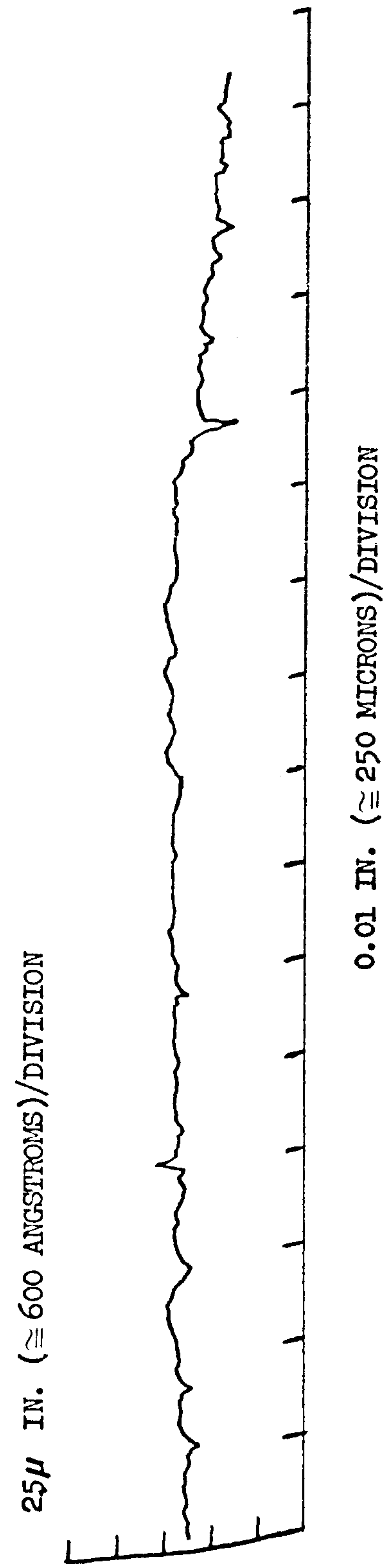

ORTHOCLASE (001)

O(//) Fl

SURFACE ROUGHNESS

ALONG a-AXIS

Figure 5

ORTHOCLASE (001)

O(//) F2

SURFACE ROUGHNESS

ALONG a-AXIS

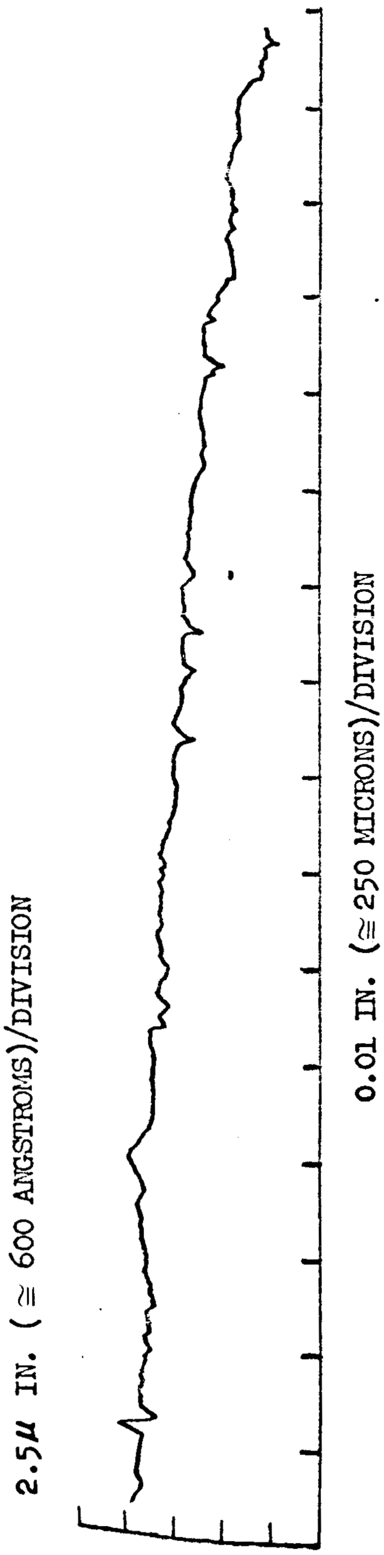

Figure 6

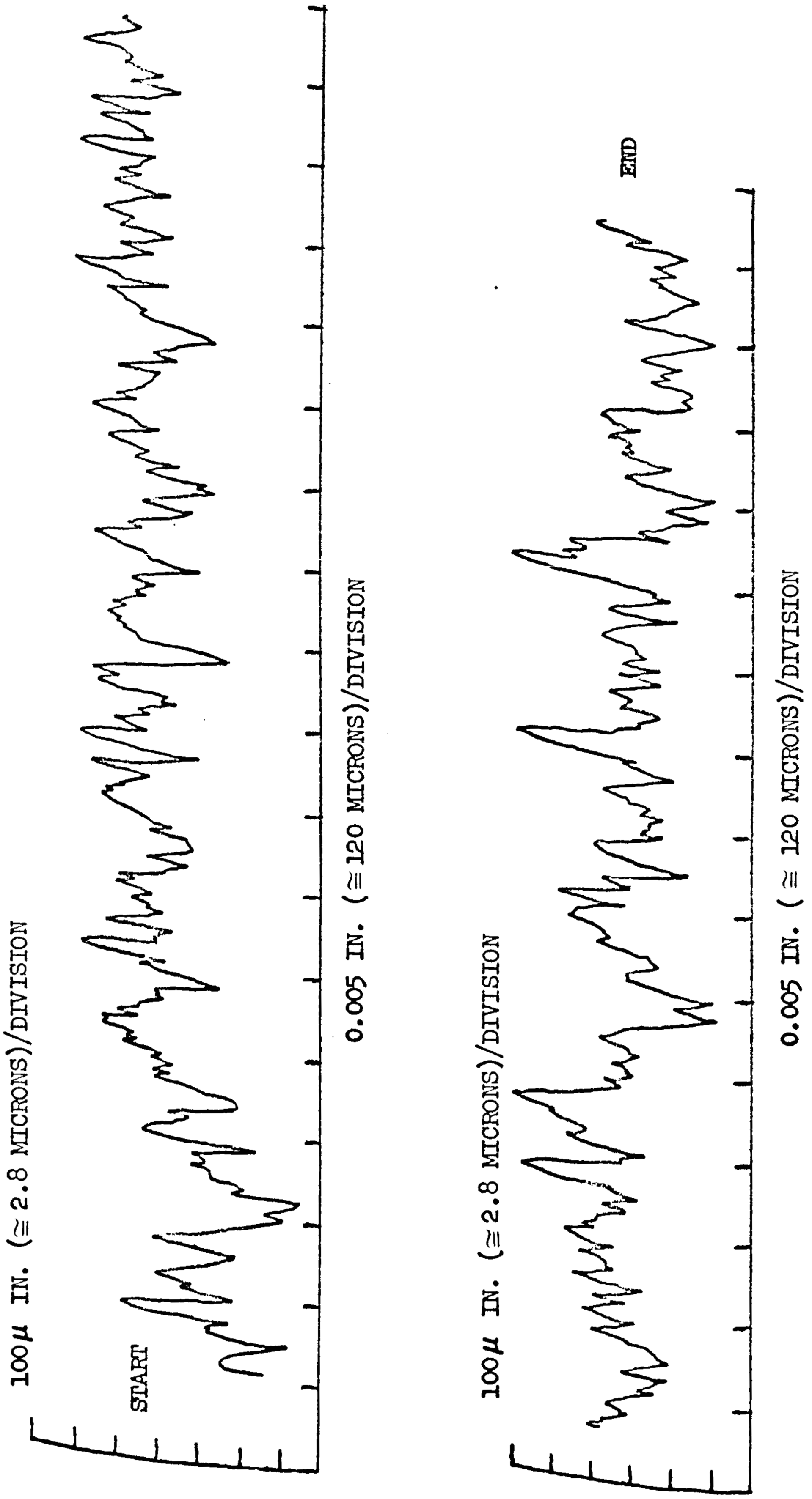

ORTHOCLASE (001)

O(/) IT

SURFACE ROUGHNESS

ALONG a-AXIS

Figure 7

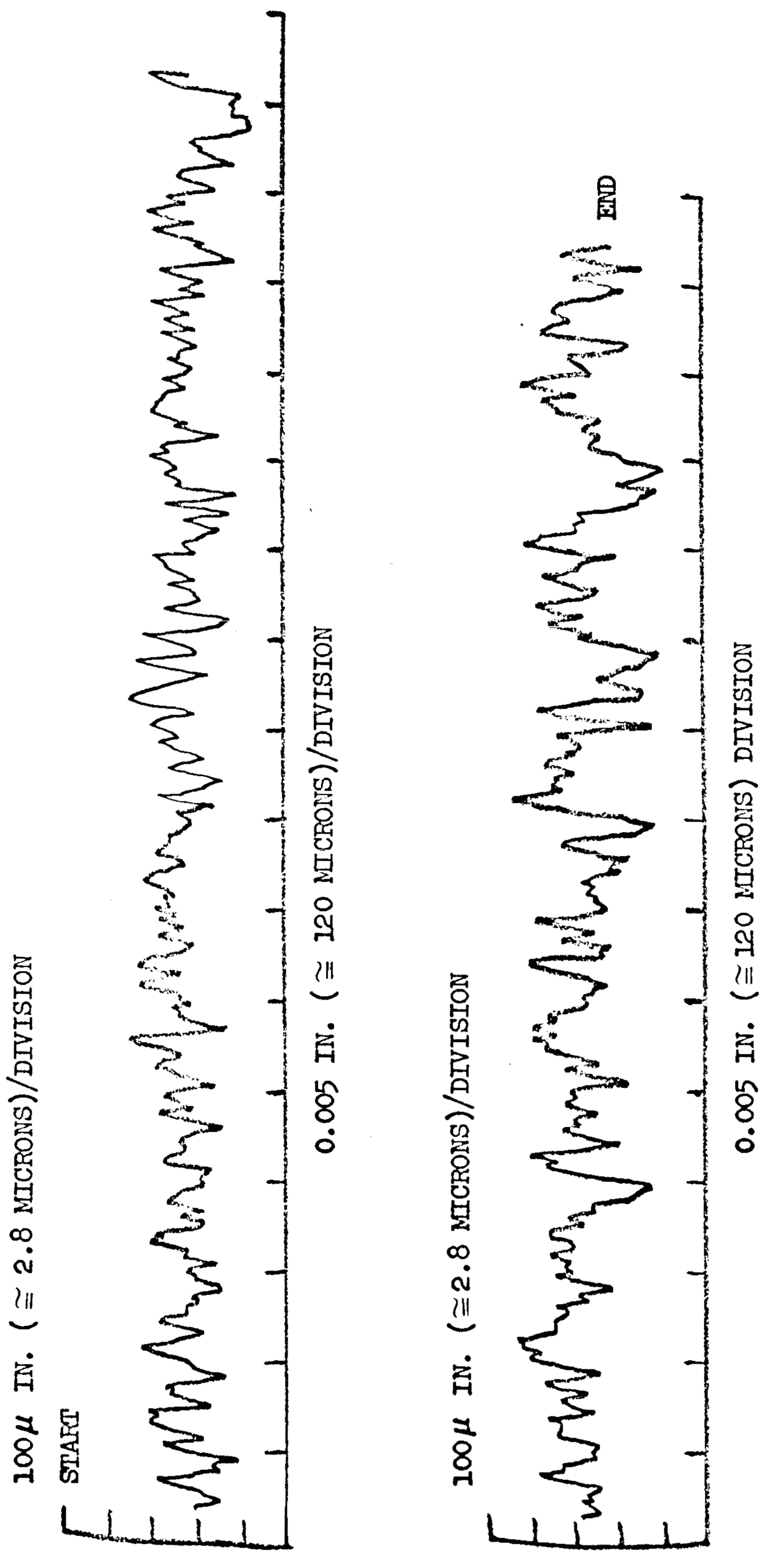

ORTHOCLASE (001)

0(∥) 1B

SURFACE ROUGHNESS

ALONG a-AXIS

Figure 8

Details of individual runs are given in the following paragraphs.

Runs #19 and #20

These runs were performed with a single pumpdown. The experimental procedure used was the same as that detailed in Reference 1 except that sorption rather than mechanical pumping was used, and the new experimental chamber was installed.

The results, for two crystalline orientations, are shown in Figure 9. There is a rather definite indication of a two branch behavior such as noted previously for other runs [though not previously for orthoclase contacting orthoclase (Reference 1)].

While at vacuum it was noted that there was measurable adhesion at zero load. In addition, a definite long range force was present, corresponding to an adhesion force of about $600\mu g$. This force was subsequently found to persist in dry nitrogen and air, in fact in air its magnitude increased to about $900\mu g$. The origin of this force has not as yet been determined, though it is suspected that one or both samples may have contained free iron inclusions. Accordingly, in Figure 9, at low load force, two branches to each curve have been drawn. The lower branch (solid) in each case represents the magnitude of the adhesion with the long range force contribution removed; for the upper branches (dashed), the long range force contribution has not been removed.

The system was then let up to atmospheric pressure with dry nitrogen. Adhesion remained, its magnitude at zero and small loading being about the same as in vacuum. A large number of attempts (about 30) were made to measure adhesion at highest load ($\cong 1000$ gm). It was found that

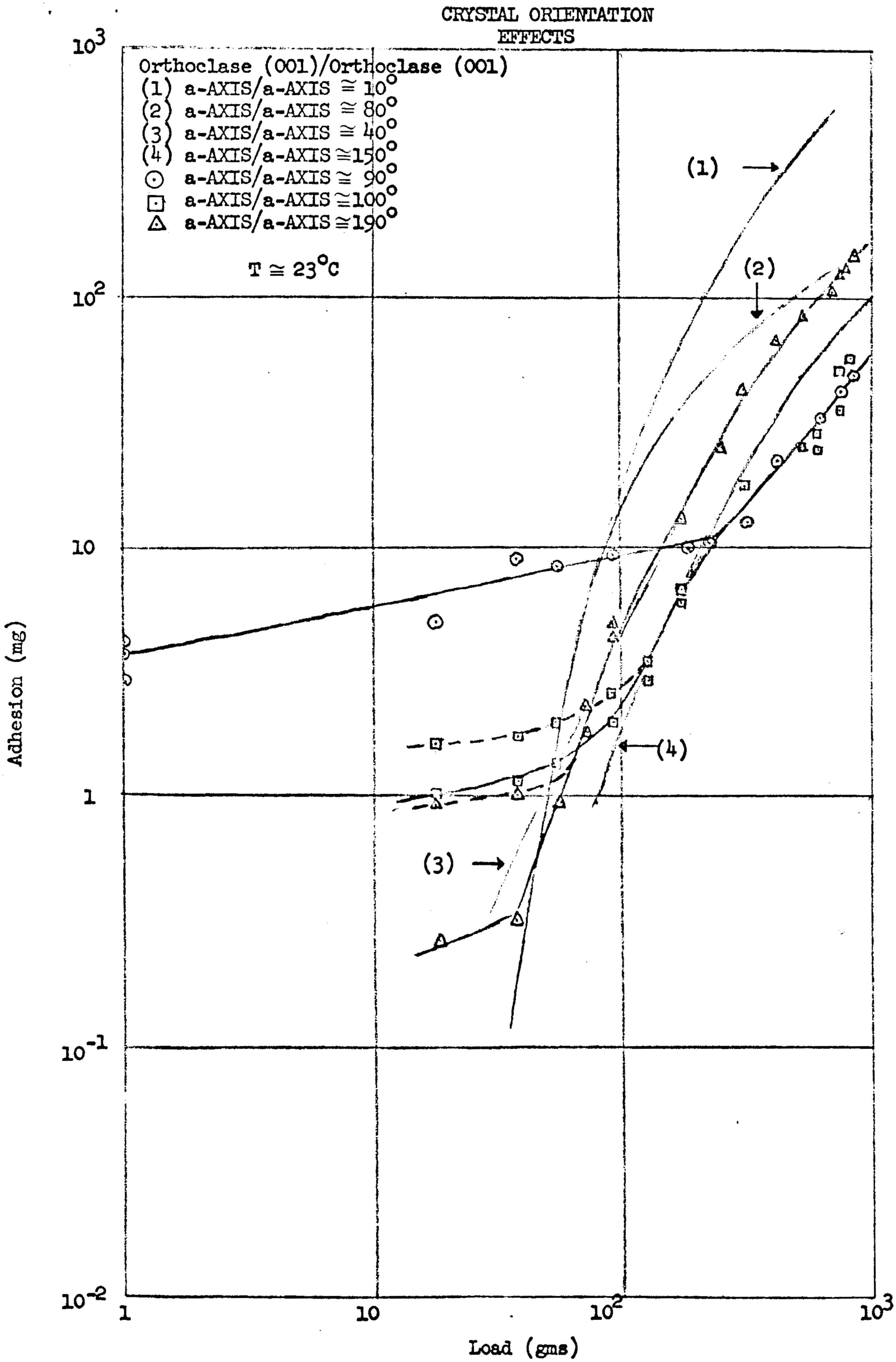
CRYSTAL ORIENTATION
EFFECTS
Orthoclase (001)/Orthoclase (001)
(1) a-AXIS/a-AXIS ≅ 10°
(2) a-AXIS/a-AXIS ≅ 80°
(3) a-AXIS/a-AXIS ≅ 40°
(4) a-AXIS/a-AXIS ≅ 150°
a-AXIS/a-AXIS ≅ 90°
a-AXIS/a-AXIS ≅ 100°
a-AXIS/a-AXIS ≅ 190°
T ≅ 23°C
(1)
(2)
(3)
(4)
10^3
10^2
10
1
10^{-1}
10^{-2}
Adhesion (mg)
1
10
10^2
10^3
Load (gms)

Figure 9

adhesion was present in all cases, generally of magnitude about one to two milligrams, but in three instances as great as ten milligrams. Though these maximum values were considerably smaller than those obtained at vacuum, they are significantly greater than any obtained previously in nitrogen.

After about five hours at dry nitrogen during which time the magnitude of the adhesion at load slowly decreased (no change was noted in the zero load adhesion), air was admitted to the system. The magnitude of the zero load adhesion immediately increased to about $900\mu g$; whereas the magnitude of the load produced adhesion immediately dropped to a value not much in excess of the new zero load value. After about one hour all indications of a load dependence disappeared, but an adhesion of about $900\mu g$ remained. It is of interest to note that this was, to the time of these runs, the "smoothest" sample pairs used (see Figures 1, 2, 3 and 4). This point is discussed in the Discussion Section (Section 3.0).

One final point, concerning the zero load adhesion, is worth noting. In vacuum, to obtain measurable values, it was necessary to have good sample parallelism. On the other hand, for the measurements in nitrogen and air it was found that the samples could be considerably out of parallel (sufficiently so for a noticeable gap on one side to be present) and yet have measurable adhesion. This is indicative of the action of very long range forces (undoubtedly due to surface charging) which, incidentally, acted to a much lesser degree in vacuum.

After these runs the samples were removed from the vacuum system and their contact surfaces studied with the petrographic microscope. Considerable surface disruption was found to be present. Micrographs of these surfaces will be included in the second annual report for this study.

Run #21

The samples used for this run were polished to be as close to optical flatness as possible (see Figures 5 and 6). The purposes of this run were (1) to determine how surface roughness affected the magnitude of the adhesion, and (2) to determine whether or not surface roughness played any role in the surface disruption and material transfer noted in previous runs (Reference 1).

The experimental procedure used was the same as that for Runs #19 and #20. The results are presented in Figures 9 and 10. The two branch behavior reported for previous runs is quite evident. In addition, the magnitude of the zero load adhesion is the highest detected for any of the runs. No long range force was detected.

The system was then let up to atmospheric pressure with dry nitrogen. Immediately thereafter, at highest load, a large magnitude adhesion (about 70 mg) was detected. Following this, a force of 10 mg was observed, again at highest load. The third measurement produced an adhesion force of 3 mg, and this remained constant, independent of load, thereafter (3 mg is slightly less than the zero load vacuum value). No long range force was detected.

The samples were then removed from the vacuum system and their contact surfaces studied with the petrographic microscope. A great amount of surface disruption was found to be present. The amount was considerably greater than noted for any of the orthoclase pairs run previously. This may, however, be an observational effect since due to the smoothness of

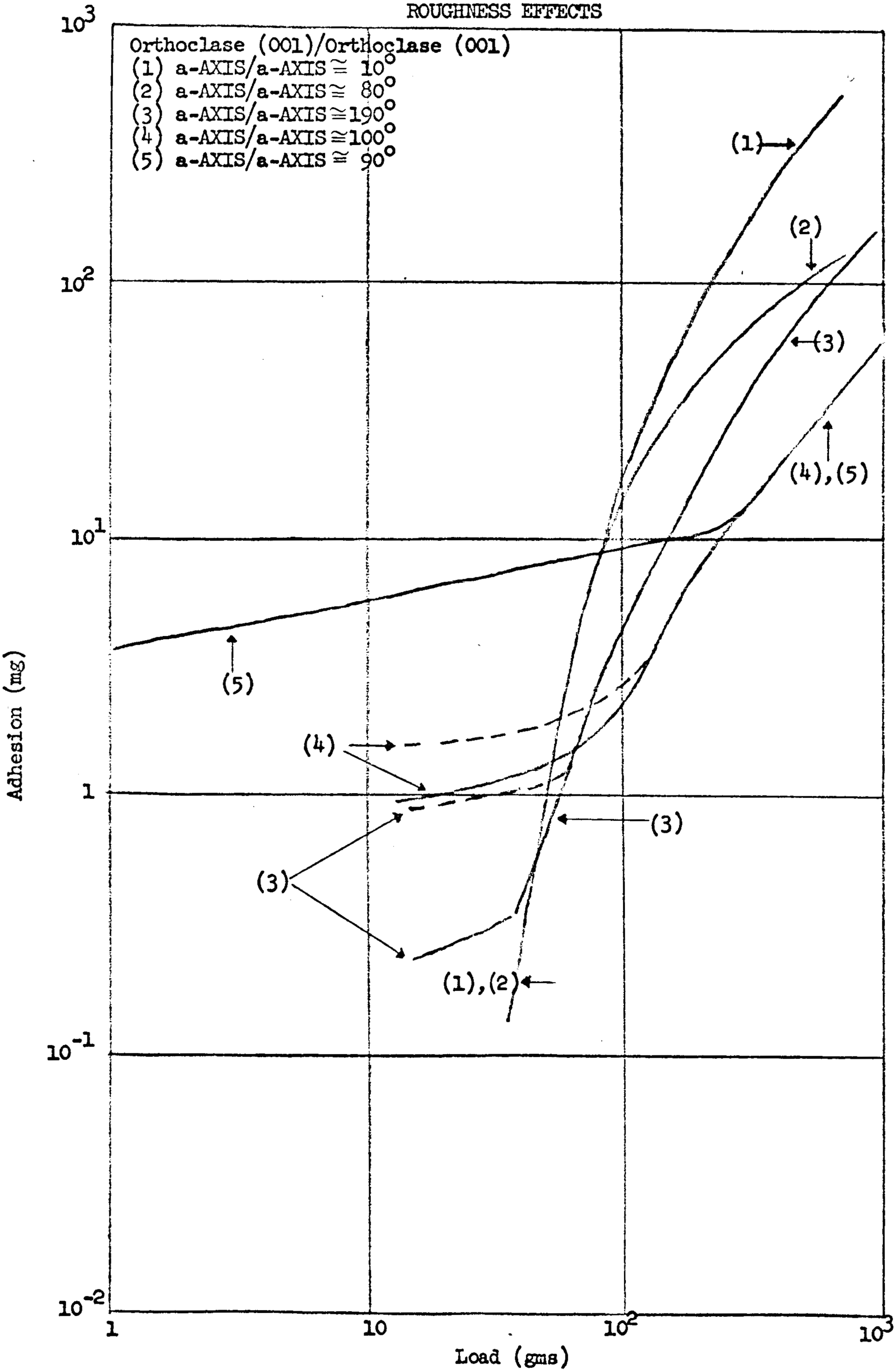

ROUGHNESS EFFECTS
Orthoclase (001)/Orthoclase (001)
(1) a-AXIS/a-AXIS ≅ 10°
(2) a-AXIS/a-AXIS ≅ 80°
(3) a-AXIS/a-AXIS ≅ 190°
(4) a-AXIS/a-AXIS ≅ 100°
(5) a-AXIS/a-AXIS ≅ 90°
(1)
(2)
(3)
(4),(5)
(5)
(4)
(3)
(3)
(1),(2)
Adhesion (mg)
Load (gms)
10^3
10^2
10^1
1
10^-1
10^-2
1
10
10^2
10^3

Figure 10

the surfaces the damage was more easily visible. Though the surfaces were similar in appearance, it was also possible to conclude that material transfer had occurred because numerous pits were evident where material had been physically removed from the surfaces (the excellent visibility allowed association between pits and deposits to become obvious). Micrographs of these surfaces, before and after the run, will be included in the second annual report for this study.

RUN #22

This run was a repeat of Run #3 reported in Reference 1. The purpose of the run was to determine the degree of reproducibility of the data.

The experimental procedure used was the same as that for Runs #19, #20, and #21. The results are shown in Figure 11. Also plotted on this figure are the results from the previous run (Run #3). Run #22, as of this time, is not complete, data having been obtained only for the higher loadings. The complete run will be reported in the next quarterly report.

3.0 DISCUSSION

3.1 Effects of Forepump Type

As noted previously, the data for this quarter were obtained using sorption pumps for initial pumpdown. These replaced the previously used mechanical pump - liquid nitrogen cold trap system. The purpose of this modification was to determine whether the mechanical pump was putting oil contamination into the ultra-high vacuum part of the system, and in particular, if it did, whether this could affect the adhesion obtained.

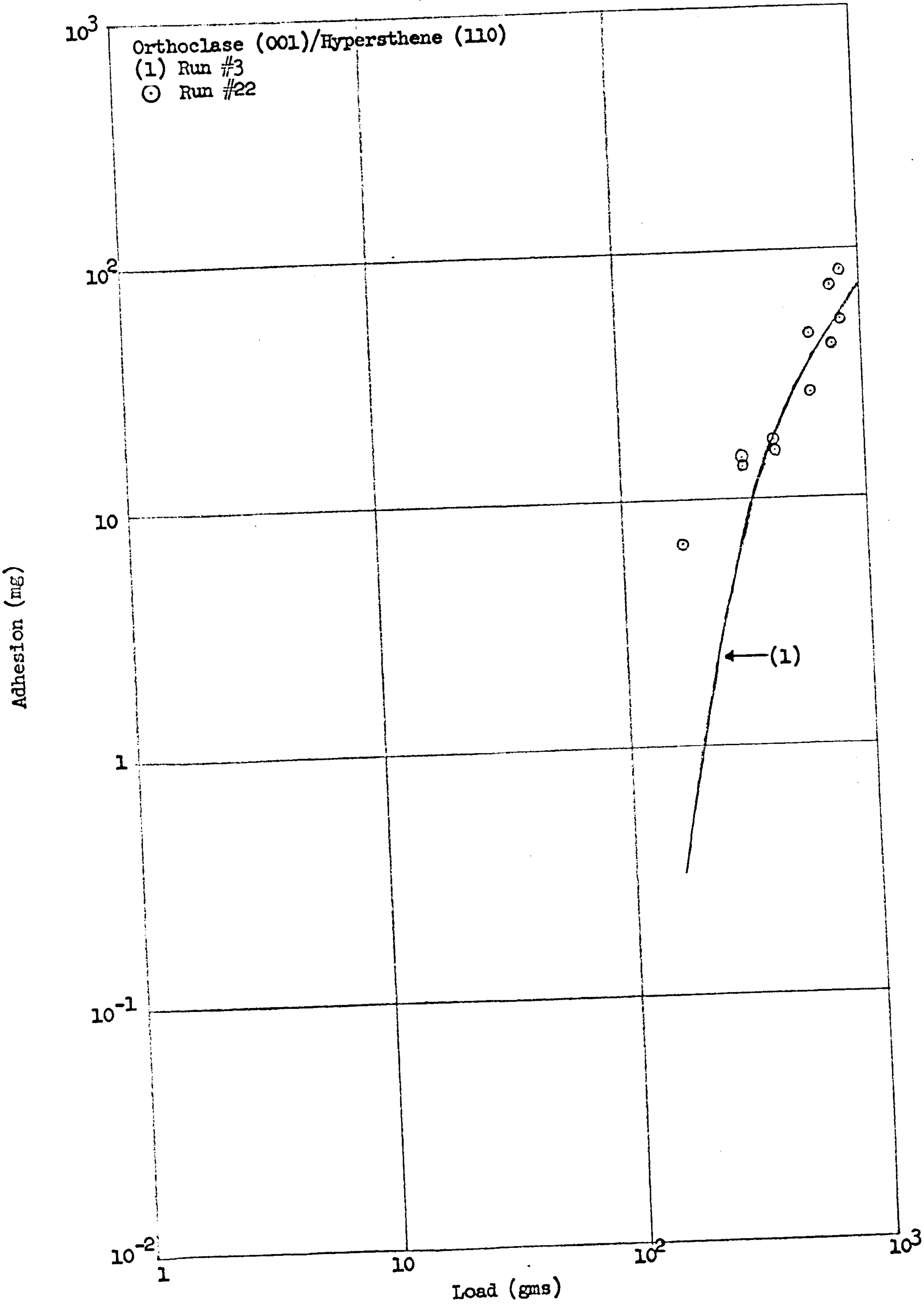

Orthoclase (001)/Hypersthene (110)
(1) Run #3
⊙ Run #22
(1)
Adhesion (mg)
10^3
10^2
10
1
10^{-1}
10^{-2}
1
10
10^2
10^3
Load (gms)

Figure 11

Prior to the sorption pump runs the vacuum system was disassembled and thoroughly cleaned.

As can be seen from the data obtained there is no indication that the type of forepump system used had any effect on the adhesion obtained.

3.2 Repeatability

Repeatability is one of the most important aspects of experimental work. This is particularly so for adhesion-friction studies since for these, in the past, repeatability has been difficult to obtain. Accordingly, it was decided to repeat some of the previous runs. To date the orthoclase (001) contacting hypersthene (110) run (Run #3 of Reference 1) has been repeated (present Run #22). The results for both runs are shown in Figure 11. As noted previously, this latest run is not as yet complete. However, it can be seen that at higher loads the data are in excellent agreement. There is some evidence of deviation at lower loads; but more data are required to substantiate this.

3.3 Orientation Effects

The studies to date relating to orientation effects are summarized in Figure 9. Of interest are the high load sections of the curves since previous work has indicated strongly that the behavior shown at high load is due to the action of the normal atomic bonding forces (ionic-covalent), and these may show crystalline orientation effects.

Data have been obtained for the (001) faces of orthoclase with various orientations of the respective a-axes (e.g. 10°, 40°, 80°, 90°, 100°, and 190°). The highest magnitude adhesions are found for the 10° orientation, i.e., for the orientation closest to atomic match across the interface. The lowest adhesions are found for the two runs where the a-axes are 90° and 100° out of match. As the orientation approaches 180° the adhesion increases again ($190^\circ > 150^\circ > 90^\circ$ and 100°), though not to the level attained for the 10° orientation. This behavior is consistent with an orientation effect associated closely with crystal structure, and gives additional evidence that the normal bonding forces are indeed responsible for this high load adhesion.

There is, however, one serious problem remaining. This pertains to Curve (2), for the 80° orientation. To fit in with the picture outlined above this curve should fall close to the 90° and 100° curves, i.e., for this orientation the adhesion should be lowest. However, to the contrary, the curve falls above all the other curves except the 10° curve. The reason for this is not presently clear. Hence, it will be necessary to obtain additional curves. In particular all orientations will be run using a given sample pair. The curves shown here were obtained with four different sample pairs having different surface roughnesses.

3.4 Roughness Effects

The data obtained to determine the effects of surface roughness upon adhesion are shown in Figure 10. Curves (1) and (2) were obtained from the roughest surfaces (see Figures 7 and 8 for the roughness plots); Curves (3) and (4) were obtained from surfaces of intermediate roughness (see Figures 1-4); while Curve (5) was obtained from surfaces which were made as smooth as possible (see Figures 5 and 6).

Since different crystalline orientations were used in the runs, not much can be said at present about the effect of roughness upon the high load adhesion behavior. However, the effect of roughness upon the low load behavior is quite evident. For the roughest surfaces, as load force decreases, the magnitude of the adhesion rapidly drops below detectable. For the intermediate roughness surfaces measurable adhesion remained even at zero load. For the "optical flat" surfaces adhesion also remained even at zero load, and in addition its magnitude was considerably greater than for the intermediate roughness surfaces. This behavior is precisely what one would expect if the low load adhesion (Type B behavior of Reference 1) were caused through the action of the dispersion forces, as concluded tentatively in Reference 1.

3.5 Material Transfer

In Reference 1, it was concluded that the high magnitude adhesion observed at high load (Type A behavior) was most probably due to the action of the normal bonding forces (ionic-covalent). One of the major arguments used was the notable surface damage and material transfer that occurred each time these high magnitude adhesions were detected, and the absence of such when these were absent.

One difficulty with this argument was that this disruption and transfer could conceivably be caused simply by the effects of surface roughness (even though only normal load was applied lateral movement on a microscale due to the roughness could occur, resulting in breakage of surface asperities). Accordingly, attempts were made to reproduce this damage and transfer in air by applying normal load and rotating the samples while in contact. No damage or transfer, even remotely approaching that found in vacuum, could be obtained. This provided strong evidence that surface roughness was not responsible.

However, it could be argued that roughness was not as effective in air due to the lubricating effect of the air and associated impurities. In order to remove this uncertainty it was decided to make a vacuum run with a pair of "optical flats." These were prepared, and their surface roughness is shown in Figures 5 and 6. It can be seen that the maximum height of surface irregularities is considerably less than 600 angstroms.

High magnitude adhesion was found for these samples (Figure 9). Study of the contacting surfaces after the run showed that considerable surface damage had occurred. In fact, more damage was evident than for any previous run (this may be, however, an observational effect since, due to surface smoothness, damage was more easily visible). In addition, indications were present that extensive material transfer had occurred. This was determined by matching the surfaces to the orientation they had in vacuum and searching for (and finding) correlation across the surfaces between pits and deposits.

The results of this run indicate quite definitely that surface roughness does not play a significant role in the observed surface damage and material transfer. This finding adds strength to the previously reached conclusion that the high magnitude adhesion is caused through the action of the normal atomic bonding forces.

4.0 SUMMARY

Several equipment modifications were made during this quarter. These included the replacement of the mechanical forepump by sorption pumps, and the installation of a new experimental chamber which permits utilization of an electron gun and allows vacuum cleavage to be performed. Additionally, a device for vacuum cleaving was designed and built. Preliminary tests of this in air indicated that it performed satisfactorily.

The data obtained relate principally to (1) the effects of the type of forepump, (2) data repeatability, (3) crystalline orientation effects, (4) roughness effects and (5) surface damage and material transfer. It was found that (1) the type of forepump used had no discernible effect on the data obtained, (2) the data appeared to be reasonably reproducible, (3) crystalline orientation effects relatable to crystalline structure were present, but that further work would be required before a definitive conclusion can be reached, (4) decreasing surface roughness resulted in an increase in the magnitude of the low load adhesion, indicating that the dispersion forces were responsible for this adhesion, and (5) surface roughness was not responsible for surface damage and material transfer, thus strengthening the argument that these are produced through the action of the normal atomic bonding forces.

REFERENCE

(1) Ryan, J. A., Experimental Investigation of Ultra-High Vacuum Adhesion as Related to the Lunar Surface, Douglas Report SM-47914, dated June 30, 1965.